DOI 10.1007/s11041-024-01006-4
Metal Science and Heat Treatment, Vol. 65, Nos. 11 – 12, March, 2024 (Russian Original Nos. 11 – 12, November – December, 2023)

UDC 669.017:621.78:669.715:621.762:621.74.043:620.17-18

EFFECT OF T6 AND T6I4 AGING TREATMENTS ON MICROSTRUCTURE AND COMPRESSIVE PROPERTIES OF ALUMINUM METAL MATRIX COMPOSITES REINFORCED BY SiC_w VIA SQUEEZE CASTING

Tao Wei,[1] Xiaojing Xu,[1, 2] Bin Zhang,[1] Guoning Bao,[1] Lele Liu,[1] Shuaidi Li,[1] and Jianming Wu[1]

Translated from *Metallovedenie i Termicheskaya Obrabotka Metallov*, No. 12, pp. 49 – 58, December, 2023.

Original article submitted July 7, 2022.

The microstructure and compressive properties of the 7xxx series aluminum alloy (Al – 12.44Zn – 3.22Mg – 1.13Cu – 0.19Zr – 0.12Sr) reinforced with SiC whiskers via squeeze casting are investigated after aging treatments T6-1, T6-2, T6I4-1, and T6I4-2. For this purpose, the effect of four kinds of aging heat treatments on the properties of the aluminum metal matrix composites (AMMCs) is studied systematically through Vickers hardness and room temperature compressive testing. The microstructure is analyzed by optical microscopy, scanning electron microscopy, and x-ray diffraction. The experimental results show that the hardness of the AMMCs after four kinds of aging processes has different degrees of improvement compared to no-aging. After the T6-1, T6-2, T6I4-1, and T6I4-2 aging processes, the hardness of the composites is 325, 278, 306, and 345.8 *HV*, respectively. The additional T6-2 aging treatment provides the highest compressive strength and compressive strain, about 747 MPa and 7%, respectively, as well as a maximum dislocation strengthening of approximately 86.89 MPa.

Key words: AMMC, aging, microstructure, mechanical properties.

INTRODUCTION

Aluminum and aluminum alloys are widely used as matrices for metal matrix composites [1, 2]. Aluminum metal matrix composites (AMMCs) are generally used for high-speed and heavy-duty work environments, such as automobile parts, engine pistons, brake discs, bearings, etc. or aircraft chassis, wings, etc. in the aviation industry [3]. For critical structural components, the matrix alloys of the AMMCs are usually selected from age-hardenable alloys of the Al – Zn – Mg – Cu system (series 7xxx) and Al – Cu – Mg system (series 2xxx) [4]. These alloys present a high practical interest and should be studied with the aim to elevate the combination of their mechanical properties by heat treatment.

It has been reported [5] that the properties of aluminum alloys and AMMCs can be significantly improved by an aging treatment, especially for the 7xxx series aluminum alloys, that have an elevated tensile strength, are age-hardenable, and possess other beneficial properties [6 – 7]. The development route of the aging process can be described follows: T4 (natural aging) → T6 (peak aging) → T76 (overaging) → T77 (retrogression and re-aging) → T6I4 (interrupted aging). The authors of [8] have found that the hardness of the AMMCs reinforced with SiC particulate (SiC_p) can remain stable for a long time during the T4 aging process. The possibility of raising the fretting wear resistance of the A356 AMMC reinforced with SiC_p by a T6 aging treatment has been studied in [9]. The main negative effect of the overaging was decrease in the hardness and strength of the composites, whereas their impact toughness remained virtually unchanged. It is also known that when the aging temperature is increased, the properties of the aluminum matrix composites show a downward trend [10]. In the recent years, the authors of [11] have proposed interrupted aging (T6I4), which involves addition of a low-temperature aging stage in the middle of the traditional aging process. After the T6I4 aging treatment, the tensile properties and the fracture toughness of the alloys were improved due to refinement of inclusions of secondary phases in the structure of the alloy [12, 13]. Similarly, the cryogenic aging treatment used in

[1] Institute of Advanced Manufacturing and Modern Equipment Technology, Jiangsu University, Zhenjiang, China.
[2] E-mail: xjxu67@126.com.

TABLE 1. Hardness and Mechanical Properties of Composites Tested for Compressive Strength after Different Aging Treatments

Treatment	Temperature-time aging parameters	*HV*, kgf/mm^2	σ_c, MPa	δ, %
Initial*	–	268	–	–
T6-1	121°C, 5.0 h	325	727	5.4
T6-2	121°C, 2.5 h	278	746	7.0
T6I4-1	120°C, 4 h, water cooling + 65°C, 56 h	306	677	5.5
T6I4-2	120°C, 2 h, water cooling + 65°C, 56 h	346	666	6.2

Notations: Initial — quenching; σ_c) ultimate compressive strength; δ) degree of compressive deformation (compressive strain).

[14] has improved the microhardness and the wear resistance of the AMMC due to the changed precipitation of the strengthening phase. However, only a few publications deal with the effect theT6 and T6I4 aging treatments on the compressive strength and wear resistance of AMMCs.

Modern composite materials are commonly divided into particulate-reinforced and fiber-reinforced ones according to the type of the reinforcement. Fiber-reinforced materials can acquire different properties depending on the fiber type [15]. SiC fibers are a preferred reinforcing material for any type of matrix as compared to B_4C, TiC and B fibers [16]. SiC whiskers (SiC_w) give a fine acicular short-fiber material commonly without defects, which exists in the form of a single crystal. Aluminum composites with SiC_w reinforcement possess a high wear resistance and hardness, a low specific weight and a good processibility [17 – 19]. However, we have virtually no data on the effect of various aging modes on the AMMCs reinforced with SiC_w after pressure casting.

The aim of the present work was to study the effect of four different aging modes (T6-1, T6-2, T6I4-1, T6I4-2) on the microstructure and compressive mechanical properties of a squeeze-cast AMMC with the use of a self-melted aluminum alloy of series 7xxx as the metal matrix and SiC_w whiskers as the reinforcement.

METHODS OF STUDY

To obtain the composite material, we used a matrix component from self-melted aluminum alloy of series 7xxx containing (in wt.%) 12.44 Zn, 3.22 Mg, 1.13 Cu, 0.19 Zr, 0.12 Sr, the remainder Al. The chemical composition of the alloy was determined by the method of EDS combined with spectrum analysis. The content of the reinforcing SiC_w in the composite amounted to 25 vol./vol.%.

The alloy was melted from high-purity (> 99.97%) Al, Zn and Mg and Al – 50.12 wt.% Cu, Al – 9.89 wt.% Sr and Al – 4.11 wt.% Zr master alloys. A weighed portion of aluminum was placed into a crucible vacuum resistance furnace of type SG and melted for 2 h at 800°C. In the end of the melting, the temperature was reduced to 750°C, after which we added individually the pure metallic zinc and magnesium. To prevent burning of Zn and Mg, they were wrapped into a tin foil and quickly put into the melt, which was stirred evenly. Then the melt was held at 750°C for 15 min and enriched with hexachloroethane for degassing and removal of slag. The molten metal was poured into a mold heated preliminarily to 400°C. The ingot was homogenized at 450°C for 24 h in an RX3-30-13 resistance furnace and solution treated at 450°C, 2 h + 460°C, 2 h + 470°C, 2 h + 475°C, 2 h and quenched in water.

The composites were reinforced with SiC_w whiskers. The components were prepared and the composite materials formed in the following succession: dispersing → filtering → molding → drying → sintering. Certain-quality whickers, alcohol, deionized water, and binder were placed into a beaker. The mixture was stirred evenly by shocks in an ultrasonic stirrer for 3 h. The homogeneously dispersed suspension was poured into a device for preliminary preparation. After a three-days hold at room temperature, the preform was dried in a blast drying oven at 100°C for 24 h. The subsequent sintering was conducted in a mode of 200°C, 2 h + 400°C, 2 h + 600°C, 2 h + 800°C, 20 h. The aluminum matrix composite was obtained by pre-heating → melt casting → pouring → extruding → molding. Then the composite was subjected to a homogenizing annealing at 450°C for 24 h in an RX3-30-13 resistance furnace. The composite was heat treated in the mode of 450°C, 2 h + 460°C, 2 h + 470°C, 2 h + 475°C, 2 h + water quenching. The modes of the subsequent aging are presented in Table 1.

The microstructure of the matrix alloy and the AMMC in quenched condition was studied by optical microscopy. After the aging, the microstructure and the phase composition of the composite were analyzed by scanning electron microscopy (SEM), energy dispersive spectroscopy (EDS), and x-ray diffractometry (XRD). We also determined the Vickers hardness and the mechanical characteristics in static compressive tests at room temperature.

The metallographic specimens for studying the structure under a Nikon EPIPHON 300 optical microscope were etched in a 10% solution of NaOH and in a 30% solution of HNO_3 for 6 h at 35°C. The SEM and EDS studies were carried out using a JEOL Quata 200F microscope. The x-ray diffraction analysis was performed with the help of a D8 ADVANCE diffractometer in copper K_α radiation with wavelength 0.15406 nm at scanning angles 20 – 120° at a rate of 5 deg/min.

The hardness of the materials (*HV*) was measured for samples with diameter 10 mm and thickness 4 mm using a Vickers device at a load of 5 kg. Then we calculated the average values from the results of at least three measurements. The compressive mechanical properties were determined using a DDL 100 machine at deformation speed 0.5 mm/min at room temperature using cylindrical samples with diameter 8 mm and height 12 mm. The morphology of

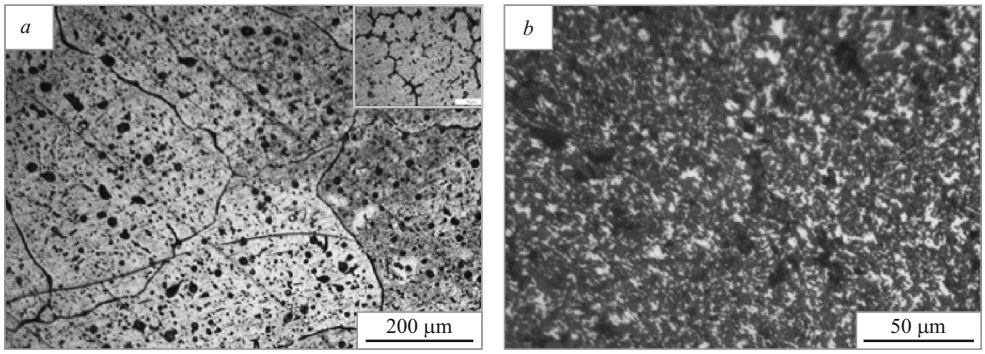

Fig. 1. Microstructure of matrix alloy (*a*) and of aluminum metal matrix composite (AMMC) (*b*) after solid solution treatment (optical microscopy).

the fracture surfaces was studied using a JEOL Quanta 200F scanning electron microscope.

RESULTS AND DISCUSSION

Figure 1 presents the microstructure of the initial matrix alloy and of the AMMC reinforced with SiC_w whiskers after the treatment for solid solution. The structure of the alloy contains coarse grains with dendritic morphology (Fig. 1*a*). In addition, the surface of the matrix alloy bears a round black region, which seems to be a manifestation of the casting porosity. The AMMC has no obvious dendritic morphology, the size of the grains of the composite material is much lower than that of the original alloy, and they a distributed in the matrix uniformly (Fig. 1*b*).

Figure 2 presents the microstructure of the AMMC after different aging modes. In all the cases, the SiC_w whiskers are distributed in the matrix uniformly. The matrix also contains agglomerates of some black particles. It can be seen (Fig. 2*a* – *d*) that SiC_w whiskers in the AMMC in state T6 have different shapes and sizes. On the contrary, the T6I4 state is characterized by a spherical or elliptical morphology of the whiskers (Fig. 2*e* – *h*). The quantitative analysis of the sizes and distribution of the whisker crystals in the matrix has shown that their size (length) is the same as that of the major axis of the original particles. The SEM measurements of over 300 precipitates in the images of the structure of the AMMC after different aging modes processed by the ImageJ software allowed us to calculate the sizes of the SiC_w crystals. It can be seen from Fig. 3 that the average size of the whiskers in state T6 (2.194 and 2.299 μm) is lower than in state T6I4 (3.393 and 2.577 μm). However, the maximum size of the whiskers in state T6 can reach 10.853 μm.

The results of the EDS analysis of the composition of the AMMS in different conditions are presented in Table 2. The main elements in the gray areas of the structure in regions *a1* (Fig. 2*b*) and *b1* (Fig. 2*d*) are Si and C. We may infer that the gray bulky material is pure SiC_w . The white-colored regions *a2* (Fig. 2*b*) and *d1* (Fig. 2*h*) bear a large content of C and Al and some Si. This means that the white regions of the structure are inclusions of Al_4C_3 precipitated during the aging. The specific contents of the elements in region *c1* (Fig. 2*f*) allow us to assume that the composite contains phases η (MgZn2) or Al – $MgZn_2$. Region *d2* (Fig. 2*h*) also exhibits a marked growth of Cu. It may be assumed that the light white particle is phase T (AlZnMgCu).

Figure 4 presents the x-ray diffraction patterns and the results of the assessment of the FWHM (full width at half maximum) of the composite material and of the matrix alloy. Analysis of the diffraction patterns shows presence of Al and SiC phases and absence of obvious peaks from other phases. This indicates absence of oxide or impurity phases in squeeze casting and good matching between the SiC_w reinforcement and the matrix alloy. Comparison of Fig. 4*b* and *c* shows that the values of the FWHM of the composite material and of the matrix alloy differ much both at high angles and at low angles. This means that the reinforcement with SiC_w changes the orientation of the crystals and the structure of the matrix of the aluminum alloy. The difference in the values of the FWHM of the composite and of the matrix alloy grows with angle θ. The FWHM of the composite attains 0.632, which indicates its high crystallinity and considerable refinement of grains and of inclusions of secondary phases in the structure. In addition, the FWHM of the composites after different aging treatments differs somewhat, which may indicate that the aging mode affects their microstructure.

We calculated the dislocation density in the composite materials using a combined Williamson and Hall model of broadening of diffraction peaks. The functional relation between these parameters and wavelength λ obtained by XRD may be described as follows:

$$\frac{(\delta 2\theta)^2}{\tan^2\theta_0} = \frac{\lambda}{d}\left(\frac{\delta 2\theta}{\tan\theta_0 \sin\theta_0}\right) + 25\langle e\rangle^2, \qquad (1)$$

where λ = 0.15406 mm; *d* is the size of the region of coherent diffraction in the XRD; $\langle e\rangle^2$ is the distortion of the crystal lattice; δ2θ is the FWHM; θ_0 is the angle of the main diffraction peaks of the alloy. Formula (1) can be used to obtain

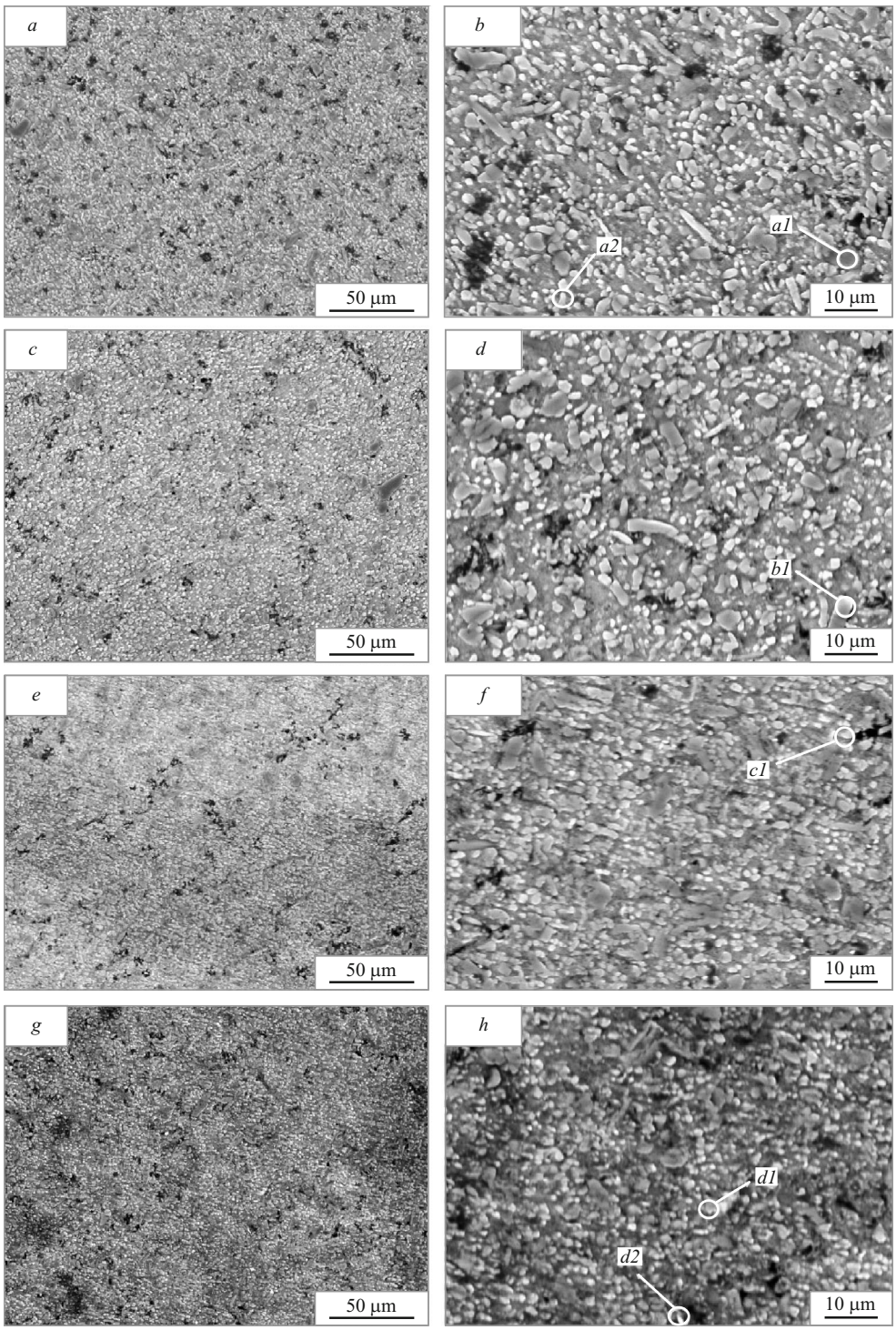

Fig. 2. Microstructure of AMMC at low (*a, c, e, g*) and high (*b, d, f, h*) magnifications (SEM) after aging by different variants: *a, b*) T6-1; *c, d*) T6-2; *e, f*) T6I4; *g, h*) T6I4-2.

the relation between $(\delta 2\theta)/(\tan\theta_0 \sin\theta_0)$ and $(\delta 2\theta)^2/\tan^2\theta_0$. The size of the region of coherent diffraction (d) and the average deformation of the lattice of the composite ($\langle e^2 \rangle^{1/2}$) can be calculated using the functional dependence given above. The relation between the dislocation density (ρ), the size of the region of coherent diffraction (d), and the average deformation of the lattice ($\langle e^2 \rangle^{1/2}$) can also be described by a function [21], i.e.,

$$\rho = 2/\sqrt{3}\,\langle e^2 \rangle^{1/2}/(d \times b), \qquad (2)$$

where b is the Burgers vector (for aluminum, $b = 0.286$ nm). The relation between the contribution σ_ρ of dislocations into

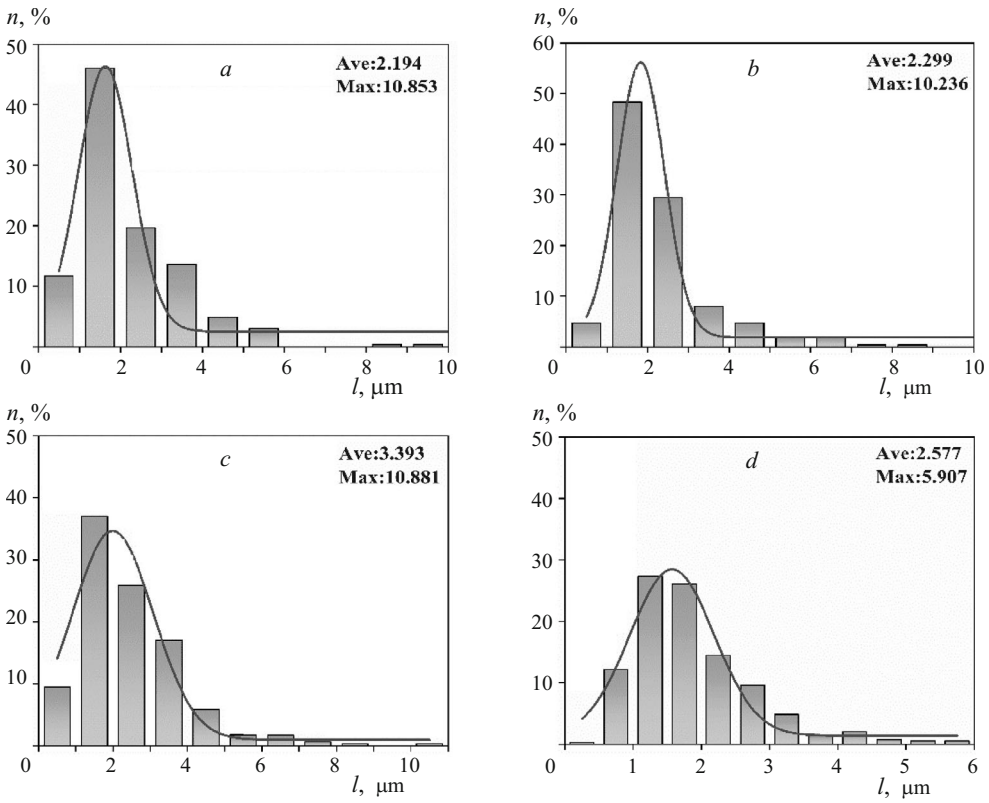

Fig. 3. Size distribution of SiC_w whiskers in the structure of AMMC after aging treatments T6-1 (*a*), T6-2 (*b*), T6I4-1 (*c*) and T6I4-2 (*d*): *n*) relative number of cases; *l*) size (length) of whiskers; Ave) averaged value; Max) maximum value.

the intensity of the hardening of the material and the dislocation density ρ is describable [22] as

$$\sigma_\rho = M\alpha G\rho^{1/2}, \quad (3)$$

where $M = 3.06$ is the Taylor orientation factor, $\alpha = 0.24$ is a numerical coefficient, and $G = 26$ GPa is the shear modulus.

The formulas and parameters presented above were used to plot the linear dependences between $(\delta 2\theta)/(\tan\theta_0 \sin\theta_0)$ and $(\delta 2\theta)^2/\tan^2\theta_0$ for the studied composites (Fig. 5). The obtained values of the slope angles and the points of intersection of the linear approximation were used to calculate the dislocation densities and their contributions into the hardening of the AMMC is different states (Table 3).

The dislocation density in the structure of the composite aged by treatment T6 attains 2.53×10^{14} m^{-2}. This is higher than in the composite in state T6I4 (1.82×10^{14} m^{-2}). Therefore, the dislocation hardening of the AMMC aged by treatment T6 is higher than that obtained after treatment T6I4. For example, after the aging treatment T6-2, the hardening is 86.89 MPa.

Table 1 presents the values of the hardness of the AMMCs before and after different aging treatments. It can be seen that the aging raises the hardness of the composites and its value depends on the mode of the heat treatment. The highest hardness corresponds to the aging by variant T6 and is equal to 325 *HV*, which is 17% higher than the hardness of the not aged composite. After the T6I4-2 aging treatment, the hardness is the highest and reaches 346 *HV*. After the T6I4-1 variant, the hardness of the composite is lower, which seems to be connected with overaging of the material.

Table 1 presents the ultimate compressive strength (σ_c) of the composites aged by different variants. Figure 6 presents the stress-strain curves of the samples obtained in the compressive tests. The results show the highest values of

TABLE 2. EDS Results for Chemical Compositions of Aged Composites

Aging treatment	Region*	Content of chemical elements, at.%					
		Al	Zn	Mg	Cu	Si	C
T6-1	*a1*	3.21	0.25	0.32	0.14	50.72	44.38
	a2	45.79	3.50	2.51	0.38	15.98	31.62
T6-2	*b1*	7.23	0.37	0.61	0.18	49.27	41.40
T6I4-1	*c1*	29.87	2.77	4.58	0.35	29.90	32.30
T6I4-2	*d1*	60.00	4.49	2.78	0.45	10.61	21.49
	d2	10.12	3.23	1.11	3.57	7.81	74.04

* See Fig. 2.

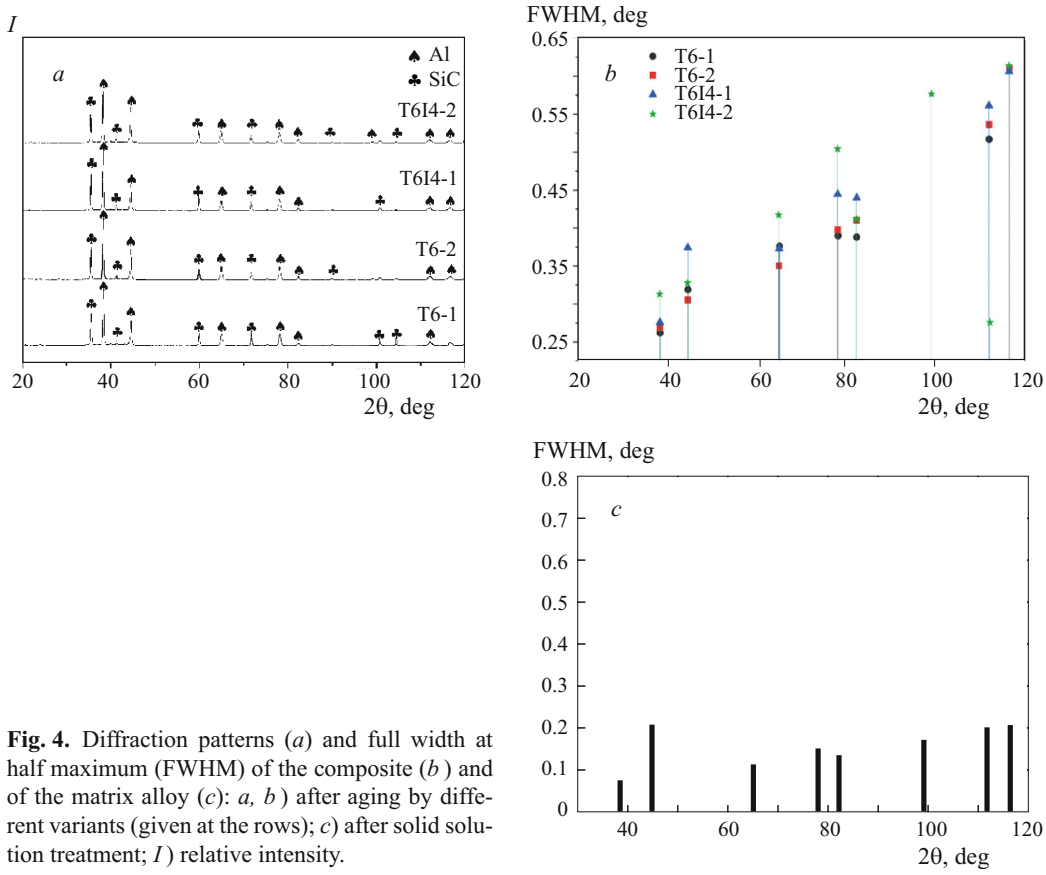

Fig. 4. Diffraction patterns (*a*) and full width at half maximum (FWHM) of the composite (*b*) and of the matrix alloy (*c*): *a, b*) after aging by different variants (given at the rows); *c*) after solid solution treatment; *I*) relative intensity.

strength and plasticity are exhibited by the composites after aging by variant T6-2 and amount to $\sigma_c = 746$ MPa at the strain at failure $\delta = 7\%$. After a longer aging (T6-1), $\sigma_c = 727$ MPa, which is lower than after the T6-2 aging treatment. The start of fracture in the stress-strain curve occurs 0.1 – 1.6% earlier than for all the other curves (Fig. 6), i.e., the plasticity of the overaged composite is low. Thus, the reinforcement of the aluminum alloy with SiC_w whiskers causes formation of a great number of fine inclusions of a hardening phase in the matrix of the composite material. This hinders the motion of dislocations in the structure and raises the compressive strength due to the dislocation strengthening without degradation of the relatively high plasticity of the composite. The results of the tests show that the T6 aging treatment provides a higher strength in the AMMC than the T6I4 aging. This seems to be explainable by the use of water cooling and especially by the longer aging time in variant T6I4. In this case the content of the precipitated hardening phase in the structure remains constant when the saturation is attained, but the morphology and the kind of distribution of the inclusions are changed. Small inclusions start to dissolve, while large inclusions start to grow, which finally lowers the strength of the composite material.

Figure 7 presents the microstructure of fracture surfaces of AMMC samples tested for compression in different states. Analysis of the morphology of these fractures allows us to infer that in all the cases, the samples fracture by a slip mechanism, which is a kind of brittle fracture. After the T6-1 and T6I4 treatments, the fracture surfaces have a concave-convex uneven pattern. After the T6-1 variant, the fracture contains a few but deep and nonuniformly distributed cracks, while the fracture morphology after the T6I4 treatment is stepped. In both cases the material has a low plasticity, i.e., 5.4% and 5.5% after the T6-1 and T6I4-1 treatments respectively (Table 1). The fracture surfaces after the T6-2 and T6I4-2 treatments bear small and evenly distributed cracks over the direction of the compression. However, the fracture surface of the AMMC after the T6-2 variant is

TABLE 3. Parameters of Dislocation Hardening of AMMC after Different Aging Treatments

Aging treatment	*d*, nm	$\langle e^2 \rangle^{1/2} \times 10^{-4}$	$\rho, \times 10^{14}, m^{-2}$	σ_ρ, MPa
T6-1	37.39	7.59	2.46	85.61
T6-2	41.30	8.63	2.53	86.89
T6I4-1	36.51	5.23	1.74	71.96
T6I4-2	40.87	6.13	1.82	73.61

Notations: *d*) size of the region of coherent diffraction in XRD; $\langle e \rangle^2$) distortion of crystal lattice; ρ) dislocation density; σ_ρ) dislocation strengthening.

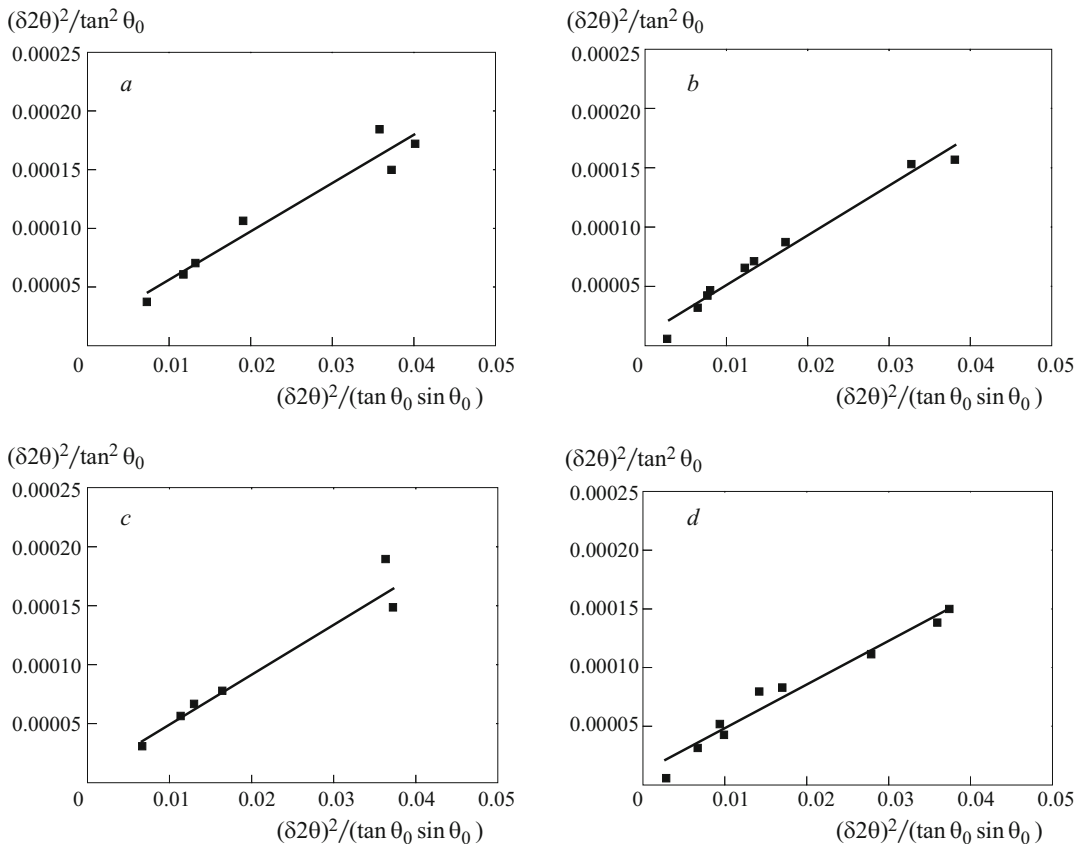

Fig. 5. Plots of linear $(\delta 2\theta)/(\tan\theta_0 \sin\theta_0)$ and $(\delta 2\theta)^2/\tan^2\theta_0$ for AMMC aged by treatments T6-1 (*a*), T6-2 (*b*), T6I4-1 (*c*) and T6I4-2 (*d*).

flat, which results in a better plasticity. The deformation to failure of the AMMC subjected to T6-2 and T6I4-2 treatments amounts to 7.0 and 6.2% respectively. Thus, the aging treatment T6-2 makes it possible to raise the compressive strength at a high enough plasticity of the studied composite.

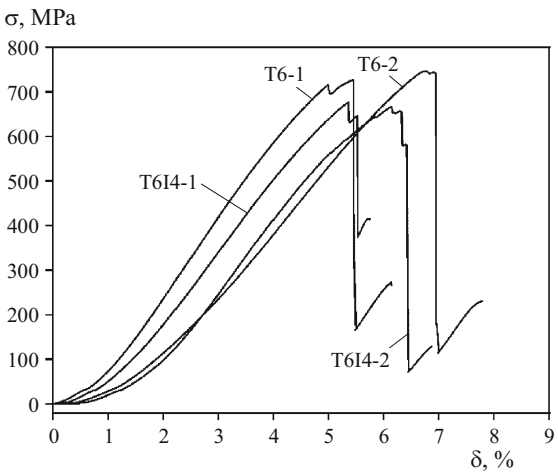

Fig. 6. Stress-strain curves in compressive tests of AMMC after different aging treatments.

CONCLUSIONS

The results of the study of the microstructure and of the compressive mechanical properties of the aluminum matrix metal composite fabricated by squeeze casting with the use of an aluminum alloy of series 7xxx (Al – 12.44Zn – 3.22Mg – 1.13Cu – 0.19Zr – 0.12Sr) as a metal matrix and SiC_w silicon carbide whiskers as a reinforcing material allow us to make the following conclusions.

1. The grain size of the composite reinforced after squeeze casting is much smaller than after the conventional production process. This is a result of the presence of the reinforcing addition in the structure, which hinders the development of secondary recrystallization. After the T6 aging treatment, the structure of the composite has a high dislocation density ($2.53 \times 10^{14}\ m^{-2}$) and the contribution of the dislocation strengthening is higher (86.89 MPa).

2. Aging elevates the hardness of the composite, but the efficiency of the treatment depends on its mode. After the aging by variants T6-1, T6-2, T6I4-1 and T6I4-2, the hardness of the composite amounts to 325, 278, 306 and 346 *HV*, respectively.

3. Aging raises the compressive strength of the composite virtually without worsening the plasticity. The T6 variant produces a higher strength than T6I4. The highest compres-

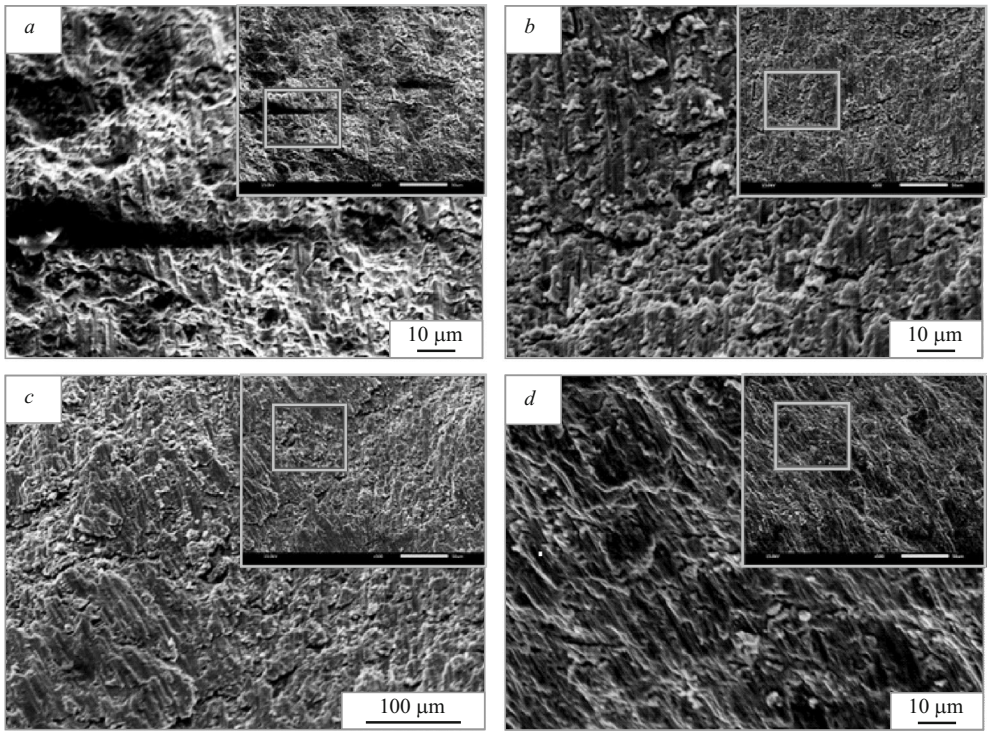

Fig. 7. Fracture surfaces (SEM) of AMMC tested for compression after aging treatments T6-1 (*a*), T6-2 (*b*), T6I4-1 (*c*) and T6I4-2 (*d*).

sive mechanical strength is provided in the composite by the T6-2 aging treatment (120°C, 2.5 h). In this case the ultimate compressive strength amounts to 746 MPa and the highest compressive fracture strain is 7.0%.

REFERENCES

1. N. K. Bhoi, D. H. Singh, and S. Pratap, "Developments in the aluminum metal matrix composites reinforced by micro/nano particles — A review," *J. Compos. Mater.*, **54**, 813 – 833 (2020).
2. C. S. Kim, K. Cho, M. H. Manjili, et al., "Mechanical performance of particulate-reinforced Al metal-matrix composites (MMCs) and Al metal-matrix nano-composites (MMNCs)," *J. Mater. Sci*., **52**, 13319 – 13349 (2017).
3. P. V. Samal, P. R. Undavilli, A. Meher, et al., "Recent progress in aluminum metal matrix composites: A review on processing, mechanical and wear properties," *J. Manuf. Process*., **59**, 131 – 152 (2020).
4. D. P. Mondal, K. Basu, S. P. Narayan, et al., "Effect of processing history and aging temperature on age-hardening kinetics of 2014-Al alloy – SiC whisker composite," *J. Mater. Sci. Lett*., **19**, 1189 – 1191 (2000).
5. S. Abarghouie and S. Reihani, "Aging behavior of a 2024 Al alloy – SiC_p composite," *Mater. Des*., **31**(5), 2368 – 2374 (2010).
6. S. Yu. Kondrat'ev and O. V. Shvetsov, "Effect of high-temperature heating on the structure and properties of aluminum alloys in the production of drill pipes," *Met. Sci. Heat Treat*., **55**(3 – 4), 191 – 196 (2013).
7. S. Yu. Kondrat'ev, O. G. Zotov, and O. V. Shvetsov, "Structural stability and variation of properties of aluminum alloys D16 and 1953 in production and operation of drill pipes," *Met. Sci. Heat Treat*., **55**(9 – 10), 526 – 532 (2014).
8. J. Guo and X. Yuan, "The aging behavior of SiC/Gr/6013Al composite in T4 and T6 treatments," *Mater. Sci. Eng. A*, **499**(1), 212 – 214 (2009).
9. C. Rong, A. Iwabuchi, and T. Shimizu, "The effect of a T6 heat treatment on the fretting wear of a SiC particle-reinforced A356 aluminum alloy matrix composite," *Wear*, **238**, 110 – 119 (2000).
10. S. Flanagan, J. Main, P. Lynch, et al., "A mechanical evaluation of an overaged aluminum metal-matrix-composite (2009 Al/SiC/15p MMC)," *Proc. Manuf*., **34**, 58 – 64 (2019).
11. R. N. Lumley, I. J. Polmear, and A. J. Morton, *Heat Treatment of Age-Hardenable Aluminum Alloys, Patent 7,025,839*, USA (2006).
12. J. Buha, R. N. Lumley, A. G. Crosky, et al., "Secondary precipitation in an Al – Mg – Si – Cu alloy," *Acta Mater.*, **55**, 3015 – 3024 (2007).
13. R. K. W. Marceau, G. Sha, R. N. Lumley, et al., "Evolution of solute clustering in Al – Cu – Mg alloys during secondary aging," *Acta Mater.*, **58**, 1795 – 1805 (2010).
14. G. R. Li, J. F. Cheng, H. M. Wang, et al., "The influence of cryogenic-aging circular treatment on the microstructure and properties of aluminum matrix composites," *J. Alloys Compd*., **695**, 1930 – 1945 (2016).
15. D. I. Zhang, G. D. Zhang, and Z. Q. Li, "The current state and trend of metal matrix composites," *Mater. China*, **29**(4), 1 – 7 (2010).
16. P. K. Jayashree, S. Gowri, S. Sharma, et al., "The effect of SiC content in aluminum-based metal matrix composites on the microstructure and mechanical properties of welded joints," *J. Mater. Res. Technol*., **12**, 2325 – 2339 (2021).

17. Z. Wang, S. Li, M. Wang, et al., "Effect of SiC whiskers on microstructure and mechanical properties of the $MoSi_2$ – SiC_w composites," *Int. J. Refract. Met. Hard Mater.*, **41**, 489 – 494 (2013).
18. W. D. Fei, Q. Y. Liu, and C. K. Yao, "Accelerating effect of whiskers on the ageing process of SiC_w/Al composite," *J. Mater. Sci. Lett*., **15**, 831 – 834 (1996).
19. Hu Wu, Zengqi Qi, Qingyan Cui, and Jian Zhou, "Research on turning process of SiC particle reinforced aluminum matrix composite brake disc," *Locomot. Rolling Stock Technol*., **06**, 20 – 22 (2021).
20. K. M. Youssef, R. O. Scattergood, K. L. Murty, et al., "Nanocrystalline Al – Mg alloy with ultra-high strength and good ductility," *Scr. Mater.*, **54**, 251 – 256 (2006).
21. Y. H. Zhao, X. Z. Liao, Z. Jin, et al., "Microstructures and mechanical properties of ultrafine grained 7075 Al alloy processed by ECAP and their evolutions during annealing," *Acta Mater.*, **52**(15), 4589 – 4599 (2004).
22. P. Luo, D. T. Mcdonald, W. Xu, et al., "A modified Hall–Petch relationship in ultrafine-grained titanium recycled from chips by equal channel angular pressing," *Scr. Mater.*, **66**(10), 785 – 788 (2012).